# Supplementary Information

for Proctor et al. "Contributions of turgor pressure, the contractile ring, and septum assembly on forces in cytokinesis in fission yeast"

**Inventory of Supplementary Information**

## Description of models

### 1- Refined estimation of force generation by the ring

We present here a more refined estimation of the pressure that the contractile ring can generate (Figure S1). The ring has a width $w$=0.1µm and a total length $2\pi R$, $R$=2µm being the radius of the cell. The force is generated by the $N$=5000/4=1250 myosin bipolar filaments, which density per unit surface is $d=N/(2\pi Rw)$, while each tetramer generates a maximum force $f$=5pN. The tension in the ring can be estimated by counting the number of tetramers intersecting the dashed line of length $w$ across the width of the ring. If b=0.3µm is the total length of the tails (the distance between the two pairs of heads), then the tetramers that can intersect the dashed line are those within a strip of length $w$ and width 2b, corresponding to a maximum number of $dwb$. The force generated by these tetramers is $dwbf$, yielding a tension $T=dbf$ in the ring. Using Laplace's law, the maximum pressure that the ring can overcome is $\sigma_{car}=T/R$, i.e.

$$\sigma_{car} = \frac{Nbf}{2\pi wR^2}, \qquad \text{(Eq. S1)}$$

which yields estimates of $\sigma_{car}$ around 750Pa. Therefore the stress that the ring can generate may be negligible with respect to turgor pressure. We also note that the total force generated by the ring is $Nbf/(2\pi R)$=0.15nN, which is comparable to previous estimates [1, 2], but slightly smaller.

### 2- Buckling length of glucan fibrils

To assess whether fibril polymerisation forces on the membrane may cause these fibers to buckle we compute the flexural rigidity of such fibers. The elastic modulus of pure beta-glucan fibers has never been reported but cellulose elastic modulus has been measured by AFM techniques to be around 150GPa [3]. The flexural rigidity, B, of such fiber is given by:

$$B = \frac{1}{4}\pi E R^4,$$

with R the radius of the fiber (R=1nm, from EM pictures [4, 5]). This yields values for B of about $10^{-25}$N.m$^2$, similar of that of a microtubule for instance. The persistence length, $L_p$ at which such a polymer will buckle because of thermal fluctuations is in turn given by [6]:

$$L_p \approx \frac{B}{kT},$$

and thus is expected to be around 30µm. Under a polymerisation forces $F_p$ of 45pN, the polymer will however buckle at a much smaller critical length, $L_B$ given by:

$$L_B \approx \sqrt{\frac{B}{F_p}},$$

and shall have typical values around 50nm.

If the fibrils are now organized in a stack made of N fibers with a radius $R_{stack}$=NR, the flexural rigidity of the stack is given by: $B_{stack}=BN^4$ and the expected buckling length of the stack by $L_{BSstack}=L_B N^2$. For a stack of 10 fibrils, this raises the expected buckling length to around 5µm. These estimations agree with data from EM pictures that depict bundles of typically 10 fibrils, which maintain a straight morphology [4, 5].

## 3- Fluctuations of the beta-glucan synthase

For a ratchet-like model to work, the distance between the polymer and the obstacle need to fluctuate in length in order for a monomer to insert at the tip. We thus computed the amplitude of the expected fluctuation of the bgs protein. The energy required to move the bgs by a distance $x$ against a force $PS_{bgs}$ is $PS_{bgs}x$, where $P$=1MPa is turgor pressure and $S_{bgs}$ is the surface of the beta-glucan enzyme. The probability that the bgs has moved more than $x$ is given by:

$$p(x) = \exp\left(-\frac{x}{h}\right)$$

with the typical amplitude of the fluctuations of the bgs position being :

$$h = \frac{kT}{PS_{bgs}},$$

which is on the order of 0.25nm. This value is slightly smaller than the size 0.5nm of a glucan monomer and the probability that the position of the bgs is compatible with the insertion of a monomer is $p$(0.5nm)=0.13. Therefore the fluctuations of the bgs are sufficient to make polymerization possible.

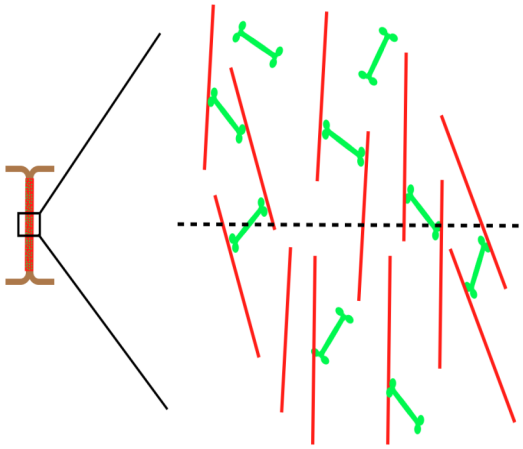

**Figure S1. Local contractile pressure generated by myosins in the ring. In support of Supplementary Model description.**

Schematic of the fission yeast ring, and close up depicting actin fibers (red) and myosins bipolar filaments (green).

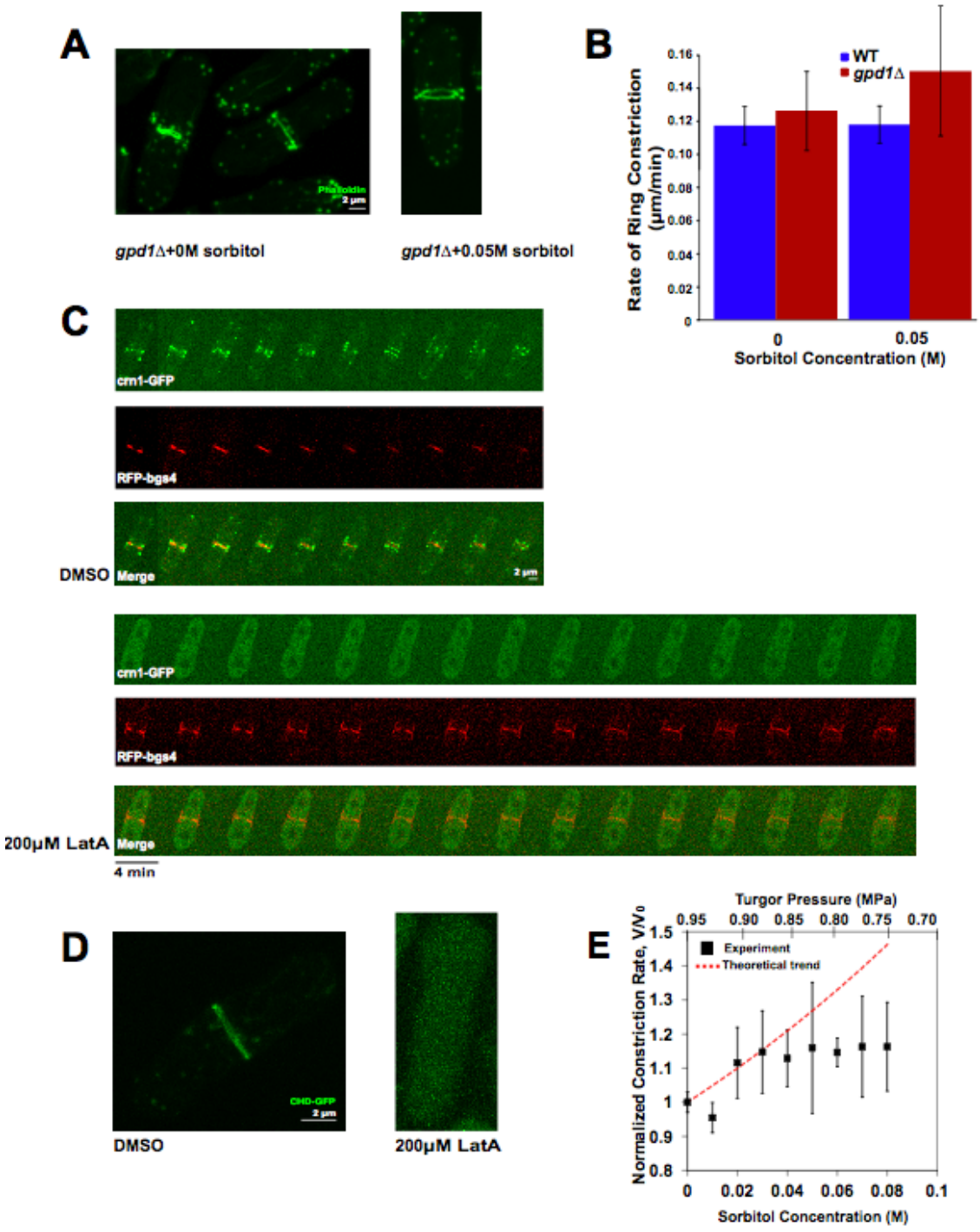


**Figure S2: Effects of sorbitol and Latrunculin A on cytokinesis. In support of Figure 1 and 2.**

A) Sorbitol does not affect F-actin in the contractile ring. *gpd1Δ* cells were treated with indicated concentrations of sorbitol for 5 min and then fixed and stained for F-actin with Alexa Fluor 488-Phalloidin. Maximum intensity projections are shown.

B) Effects of sorbitol on furrow ingression rates in WT and gpd1Δ cells. Average rates of rlc1-GFP ring closure at indicated concentrations of sorbitol. Error bars represent ± STD. These results suggest that the effect of sorbitol on cytokinesis is due to changes in turgor pressure, which is compensated for in the *gpd1*$^{+}$ cells, but not *gpd1*Δ cells.

C) 200μM Latrunculin A inhibits F-actin. Time lapse images of WT mitotic cells expressing actin patch marker crn1-GFP and septum marker RFP-bgs4 were treated with DMSO and 200μM Latrunculin A and imaged over time. Crn1-GFP patches are not present in LatA-treated cells, indicating that actin was inhibited for the duration of the experiment while the septum is ingressing.

D) Use of another marker to show F-actin inhibition by 200μM Latrunculin. CHD (Calponin-homology domain of rng2 IQGAP)-GFP is a marker for F-actin structures including the actin ring, cables, and patches. Cells expressed GFP-CHD on a multi-copy plasmid under the control on an *nmt41* promoter after induction in thiamine-less media for 12 hours. Cells were subsequently treated with DMSO or 200μM Latrunculin A for one hour and then imaged. Maximum intensity projections are shown. No actin structures were detected in the LatA-treated cell.

E) Average relative rate of ring constriction as a function of sorbitol concentration and turgor pressure: comparison between scaling predictions (red) and experiments (black; Figure 1E).

**Supplementary Table 1**

*S. pombe* strains used in this study

| Strain # | Genotype | Source |
|---|---|---|
| FC420 | *h+ ade6-M216 leu1-32 ura4-D18* | Chang Lab |
| FC2659 | *h+ rlc1-GFP:kanMX gpd1::ura4 ade6-M216 leu1-32 ura4-D18* | Chang Lab |
| FC2660 | *h- rlc1-GFP:kanMX ade6-M216 leu1-32 ura4-D18* | Chang Lab |
| FC1472 | *h- bgs4::ura4 GFP-bgs4-leu1+ leu1-32 ura4-D18 his3-D1* | JC Ribas |
| FC1470 | *h- bgs1::ura4 GFP-bgs1-leu1+ leu1-32 ura4-D18 his3-D1* | JC Ribas |
| FC2661 | *h+ cdc12-112 Pbgs4-GFP-bgs4:leu1 bgs4::ura4 ade6-M216 leu1-32 ura4-D18* | This Study |
| FC2564 | *h- myo2-E1 bgs4::ura4 GFP-bgs4-leu1+ leu1-32 ura4-D18* | This Study |
| FC2563 | *h+ cps1-191 bgs4::ura4 RFP-bgs4-leu1+ ade6- leu1-32 ura4-D18* | This Study |
| FC2559 | *h+ crn1-GFP bgs4::ura4 RGP-bgs4-leu1+ ade6-M210 leu1-32 ura4-D18* | This Study |
| FC2657 | *h- rlc1-mRFP::natR leu1 ura4* | J Moseley |
| FC2662 | *$h^{90}$ Pbgs4-GFP-bgs4:leu1 bgs4::ura4 + gpd1::ura4 leu1-32 ura4-D18* | This Study |
| FC2663 | *h- Pbgs1-GFP-bgs1:leu1 bgs1::ura4 + gpd1::ura4 ade6 leu1-32 ura4-D18* | This Study |

**Supplementary Movie**

**Movie 1. Cytokinesis without F-actin.** In support of Figure 2.

Confocal images of a fission yeast cell expressing GFP-bgs4 (a marker for glucan synthase on the plasma membrane) treated with 200μM Latrunculin A. In this condition, cells exhibit no detectable F-actin structures. Time frame is every 2 min for 30 mins. Note that the cleavage furrow ingresses in the absence of actin.

## Supplementary Materials and Methods

### Yeast strains and media

Standard methods for media and genetic manipulation were used. *S pombe* strains used are listed in Supplementary Table 1. Alexafluor 488-Phalloidin (Molecular Probes) was used for F-actin staining [7]. DAPI was added at a concentration of 1μg/mL. Cells were grown at 25°C in mid-exponential phase and imaged at room temperature (23°-26.5°) unless otherwise indicated.

### Image analysis and microscopy

A spinning-disk confocal fluorescent upright microscope, a Yokagawa spinning-disc confocal inverted microscope with a Hamamatsu EM-CCD camera, and an inverted wide-field fluorescence microscope outfitted with a motorized stage (Ludl) and Hamamatsu Orca were used for acquisitions. Temperature was controlled using an objective heater (Bioptechs). Image acquisition was performed using Micromanager 1.3 Software or OpenLab 5.0.2 (Improvision, Coventry, UK). Images were analyzed using either ImageJ (National Institute of Health, Bethesda, MD) or OpenLab 5.0.2.

### Assay for sorbitol effects

*gpd1Δ* or *gpd1*$^{+}$ cells were grown to mid-exponential phase at 25° in YE5S media without sorbitol. Sorbitol in 0.5M or 0.1M stock solutions in YES was added to the final indicated sorbitol concentrations. The consequent change in effective turgor , $\Delta P$, was computed as $\Delta P = C_s RT$, with $C_s$ the sorbitol concentration, R the gas constant and T the temperature. 500μL cultures were incubated in a 25° water bath shaker for 5 min, then concentrated for centrifugation of 20-30 sec at 5000 rpm, and 1 μl of concentrated culture was added to each slide and mounted in media with no agar pad. Ring closure rates were assayed by imaging rlc1-GFP expressing cells in the medial focal planes, which was determined by the plane exhibiting a maximum distance between rlc1-GFP foci. Constriction rates were determined manually by the maximum distance between rlc1-GFP foci as a function of time, and then fit to a linear least squares regression. Because of possible small variations such as temperature and culture conditions, we compared the rates of sorbitol-treated cells and control cells imaged on the same day and considered the rates normalized to the control rates ($v/v_0$) taken on the same day. Ratios of rates were then averaged over all days of acquisition for a given concentration of sorbitol.

### Latrunculin A assay

500-1000μl of cell culture were concentrated, and re-suspended in YE5S media. 99 μl of concentrated culture was mixed with 20mM LatA stock in DMSO for a final concentration of 200 μM solution. One μL of concentrated culture was added to each slide, covered with a coverslip and imaged. Cells presenting any degree of septa fluorescence were assayed for approximately 40 minutes via time-lapse microscopy at the medial focal plane. If the GFP signal came together in the center of the medial plane, the cell was determined to have completed septation. If septa arrested or septated to some small degree, yet failed to complete the process in the 40 min period, cells were determined to have failed septation. Most cells

that failed in septation completely in this assay arrested in the process, i.e. they displayed no centripetally directed movement of GFP signal. There was a small subset of failed cells that displayed some small degree of septum ingression, yet ultimately failed to complete septation by 40 min.

**Assaying temperature sensitive mutants**

Temperature sensitive cells (*cps1, cdc12, myo2* mutants) expressing either GFP-bgs4 or RFP-bgs4 were grown in mid-exponential phase at 25°C degrees. Dividing cells were screened visually for signal at the medial cortex. Cells were shifted to 36°C over about a 10 min period using an objective heater. We considered t=0 when the objective heater measured 36°C. Cells were determined to have completed or failed septation based on whether they arrested in septation or completed the process during the 40 min acquisition period. Unlike LatA-treated WT cells, *cps1-191* at 36°C presented no sub-population of cells that appeared to both arrest and ingress in the 40 min acquisition period; cells either arrested or continued septation. Rates of septation were determined by tracking the distance between the centripetally directed tips of the septa in the medial focal plane.

**Measuring fluorescence intensity**

Rlc1-mRFP fluorescence in the ring was measured in maximum intensity image projections, using regions of interest that encompass >95% of fluorescence intensity. The intensity of bgs proteins was measured in a region at the leading edge of the septa in the medial focal plane (up to 3 pixels away from the septa tips). Numbers of mRFP-bgs4 in nascent septa were estimated by comparing their intensity measurements to those of rlc1-mRFP in the ring [1], and with comparing GFP-bgs1 with GFP-bgs4. These estimates use the assumption that mRFP and GFP fusions are expressed equally in the ring.

**Supplementary references**


1. Wu, J.Q., and Pollard, T.D. (2005). Counting cytokinesis proteins globally and locally in fission yeast. Science 310, 310-314.
2. Zumdieck, A., Kruse, K., Bringmann, H., Hyman, A.A., and Julicher, F. (2007). Stress generation and filament turnover during actin ring constriction. PLoS One 2, e696.
3. Iwamoto, S., Kai, W., Isogai, A., and Iwata, T. (2009). Elastic modulus of single cellulose microfibrils from tunicate measured by atomic force microscopy. Biomacromolecules 10, 2571-2576.
4. Osumi, M. (1998). The ultrastructure of yeast: cell wall structure and formation. Micron 29, 207-233.
5. Osumi, M., Konomi, M., Sugawara, T., Takagi, T., and Baba, M. (2006). High-pressure freezing is a powerful tool for visualization of Schizosaccharomyces pombe cells: ultra-low temperature and low-voltage scanning electron microscopy and immunoelectron microscopy. J Electron Microsc (Tokyo) 55, 75-88.
6. Elbaum, M., Kuchnir Fygenson, D., and Libchaber, A. (1996). Buckling microtubules in vesicles. Phys Rev Lett 76, 4078-4081.
7. Chang, F., Woollard, A., and Nurse, P. (1996). Isolation and characterization of fission yeast mutants defective in the assembly and placement of the contractile actin ring. J Cell Sci 109 (Pt 1), 131-142.